Correlation of Yield Strength with Internal Coherency Strains for Age-Hardened Cu-Ni-Fe Alloys

S. D. DAHLGREN

The maximum yield strengths for a given aging temperature were measured for age-hardened Cu-Ni-Fe alloys. The yield strengths were found to be proportional to the difference in cubic lattice parameters of unstressed precipitating phases and independent of other factors such as precipitate particle size and precipitate volume fraction. The yield strength dependence on lattice parameter differences alone indicated coherency stresses controlled the yield strengths. An analysis of the yield strength based only on internal coherency strains and stresses subsequently led to the derivation of an equation for the yield strength, *i.e.*,

$$\sigma_{\text{yield}} = \frac{\overline{m}}{3\sqrt{6}} (C_{11} + C_{12} - 2C_{12}^2/C_{11}) \frac{\Delta a}{a_0},$$

where $\overline{m}$ is the Taylor factor for converting from single crystal shear stress to polycrystalline tensile stress results, C_{ij} are single crystal elastic stiffness constants and Δa is the difference in, and a_0 the average of the cubic lattice parameters of the precipitating phases. The equation indicates the yield strength is dependent only on the internal coherency strains and independent of particle size and precipitate volume fraction, as observed. The correlation of the experimentally measured yield strengths with the equation was quite good.

THE dependency of yield strength on precipitate size and spacing, precipitate volume fraction, and internal coherency stress magnitude was investigated experimentally for age-hardened Cu-Ni-Fe alloys. Precipitate size and spacing depended on time at the aging temperature,[1,2] precipitate volume fraction was controlled by alloy composition, and the magnitude of the internal coherency stresses depended on the relationship between precipitate lattice parameters and precipitate compositions.[1,2] The compositions, and thus the coherency stresses of the precipitate phases, depended on aging temperature as indicated by the increased solubility of both phases with increased temperature shown by the miscibility gap in the suido-binary phase diagram constructed parallel to the tie lines through the Cu-Ni-Fe alloy compositions investigated. The age-hardened Cu-Ni-Fe alloys contained coherent Ni-rich and Cu-rich phases[3] that were in the form of alternating tetragonally-strained platelets.[3,4] Coherency requirements caused the two normally fcc phases to have tetragonal crystal structures with c/a lattice parameter ratios <1 for the Ni-rich phase and >1 for the Cu-rich phase. Platelets were parallel to the three {100} cube planes. A model[5,6] was used to correlate the yield strength with the internal coherency strains that were produced by aging.

YIELD STRENGTH MEASUREMENTS

Solution treated, quenched and aged Cu-Ni-Fe alloys were tested in tension to determine the yield strength as a function of aging time, precipitate volume fraction and aging temperature. Four compositions were tested (Fig. 1 and Table I). Compositions 1, 2 and 3 were picked to lie on a common tie line so that the effect of volume fraction could be investigated for a given aging temperature without changing the compositions of the two precipitate phases (Fig. 1). The composition for Alloy 4 also can be designated $Cu_{10}Ni_7Fe_3$.

The alloys were cast into 1/2 in. (13 mm) diam copper molds under an inert atmosphere. Alloys 1 to 3 were forged and Alloy 4 was swaged to 3/8 in. (10 mm) diam rods and homogenized for 3 days at 950°C in evacuated quartz capsules. Tensile samples with a gage length of 28.6 mm and gage diameter of 4.1 mm were ground from the homogenized rods. The tensile samples then were solution heat treated at 950°C in evacuated quartz capsules and quenched in water prior to age-hardening heat treatments. Prior to melting, 0.5 wt pct Mn was added to each alloy to aid fabrication. The average grain size of the homogenized tensile samples was 0.15 mm.

The effect of aging time on yield strength was observed for Alloy 2 for aging times from 15 min to 200 h at 625°C. Rockwell hardness measurements also were made on the tensile samples to determine

Table I. Compositions and Precipitate Volume Fractions for Alloys 1 to 4. The Volume Fractions for the Ni- and Cu-Rich Phases were Obtained from the Phase Diagram and are Given by f_1 and f_2, Respectively

	Composition, At. Pct			Volume Fraction	
Alloy	Cu	Ni	Fe	f_1	f_2
1	54.4	36.7	8.9	0.25	0.75
2	41.8	44.8	13.4	0.50	0.50
3	30.7	52.5	16.8	0.68	0.32
4	50	35	15	0.43	0.57

S. D. DAHLGREN is Research Associate, Materials Department, Battelle-Northwest, Richland, WA 99352.

Manuscript submitted January 5, 1976.

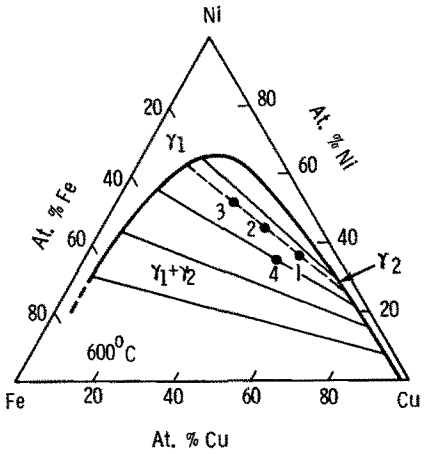

Fig. 1—Isothermal section of the Cu-Ni-Fe phase diagram for 600°C (Ref. 7). Numbers 1 to 4 designate alloy positions used in this investigation. The Ni-rich phase is given by γ_1 and the Cu-rich phase is given by γ_2.

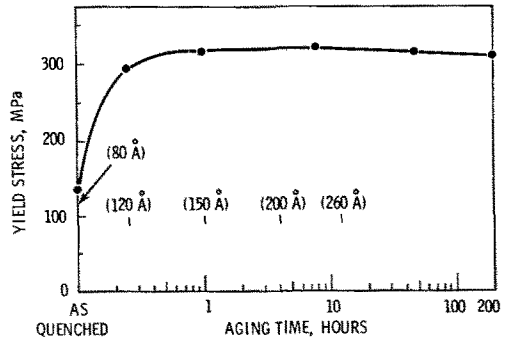

Fig. 2—Tensile yield strength *vs* aging time at 625°C measured for Alloy 2. Numbers in parenthesis designate the modulation wavelength, *i.e.*, thickness of Ni-rich and Cu-rich platelet pairs. The modulation wavelength was measured by M. Hillert, *et al*[8] for the same alloy composition and for the heat treatment times shown.

Table II. Measured Yield Strengths for Alloys 1 to 3 Aged to Maximum Hardness at 625 and 450°C

Aging Temperature, °C	Yield Strength, MPa		
	Alloy 1	Alloy 2	Alloy 3
625	325	325	330
450	440	435	435

whether or not maximum hardness occurred for the same aging time as maximum yield strength.

The effects of precipitate volume fraction and heat treatment temperature on yield strength were observed for Alloys 1 to 3, and the effect of heat treatment temperature was studied for Alloy 4. Two tensile samples each of Alloys 1 to 3 were aged to their maximum yield strength at 625°C. One sample of each alloy was tensile tested after aging at 625°C and the other sample was aged an additional 100 h at 450°C prior to tensile tests. The sequential heat-treatment permitted the precipitate size and spacing to be developed at the higher temperature and the precipitate compositions and thus the magnitude of the coherency strains to be developed at the lower temperature. Individual tensile samples of Alloy 4 were aged to maximum yield strength at 800, 730, and 625°C. An additional Alloy 4 sample was aged to maximum yield strength at 625°C to fix the precipitate size and heat-treated an additional 100 h at 550°C to establish the magnitude of the coherency strains. All samples were tensile tested at a strain rate of 0.0175 cm/cm/min. Yield strengths were determined by the 0.02 pct-offset-strain method.

Table III. Measured Yield Strengths for Alloy 4 Samples Aged to Maximum Hardness at Temperatures from 550 to 800°C

Aging Temperature, °C	Yield Strength, MPa
800	200
730	280
625	370
550	430

YIELD STRENGTH RESULTS

The tensile test results showed that the yield strength depended only on the heat treatment temperature, Fig. 2, Tables II and III. The yield strength was not at all sensitive to either aging time (*i.e.*, particle size and spacing) or precipitate volume fraction for the volume fractions studied (Table I). Samples of Alloy 2 that were aged for times from 1 to 200 h at 625°C had yield strengths that differed by only 15 MPa, and the sample aged for 15 min was only 25 MPa below the maximum yield strength of 325 MPa (Fig. 2). The modulation wavelength (Fig. 2) increased from 120 to 260Å for aging times from 15 min to 12 h, and because platelet thicknesses for Alloy 2 were about half the modulation wavelength, the yield strength therefore was nearly independent of platelet thickness for platelets 60Å to over 130Å thick. Rockwell hardness results on the Alloy 2 tensile samples showed the same trends with aging time as the yield strength results. Thus, to reduce the number of tensile tests, aging time to maximum hardness was used to determine the aging times to maximum yield strength for the remaining tensile test samples.

Maximum yield strengths for Alloys 1 to 3 were independent of volume fraction within the accuracy of the measurements, but they were clearly dependent on aging temperature (Table II). Alloys 1 to 3 aged at 625°C all had maximum yield strengths of 325 MPa, and they had maximum yield strengths of 435 MPa when aged at 450°C (Table II). A sample aged at 625°C and 450°C was aged again at 625°C for a short time. The hardness of the sample returned to that measured for a sample given only a 625°C aging treatment, *i.e.* the effect of the 450°C aging treatment was completely removed by reheat-treating at 625°C.

Maximum yield strengths of Alloy 4 tensile samples also showed a dependency on aging temperature (Table III). Yield strengths varied from 200 MPa for 800°C to 430 MPa for 550°C.

COHERENCY STRESSES AND PLASTIC FLOW

The difference in the cubic lattice parameters of the two precipitating phases decreases with increasing aging temperature as the compositions of the two precipitating phases change, so the results indi-

cate the yield strength is dependent only on the magnitude of the internal coherency strains. Any analysis of the yield strength also must account for the independence of yield strength on volume fraction and precipitate size.

Assuming the tetragonal crystal structures for the coherent Ni-rich and Cu-rich platelets were due to elastic strains, the Ni-rich phase would be stressed in biaxial tension and the Cu-rich phase would be stressed in biaxial compression. The biaxial stress in the x and y directions in an individual platelet parallel to the x-y plane was derived previously[5] to be

$$\sigma_{xx} = \sigma_{yy} = (C_{11} + C_{12} - \frac{2C_{12}^2}{C_{11}})\, e_{xx}, \qquad [1]$$

where C_{ij} are elastic stiffness constants and e_{xx} is the strain in the x direction. Thus,

$$e_{xx} = \frac{\bar{a} - a_0}{a_0}, \qquad [2]$$

where $\bar{a}$ is the "a" lattice parameter common to the two coherent phases and a_0 is the cubic lattice parameter for the unstrained phase under consideration. The stress σ_{zz} normal to the platelets was assumed[5] to be zero for the derivation of Eq. [1].

Shear stresses resolved from the biaxial coherency stresses on the slip plane in the direction of an $\mathbf{a}/2[10\bar{1}]$ Burgers vector were derived[5] to be $\tau = \sigma_{xx}/\sqrt{6}$ for either Ni-rich or Cu-rich platelets oriented parallel to (001) planes, $\tau = -\sigma_{xx}/\sqrt{6}$ for (100) platelets, and $\tau = 0$ for (010) platelets. The shear stress was zero for (010) platelets because the Burgers vector was parallel to the plane of the platelets.[5,9] Unless the platelets are oriented for zero shear stress, the shear stress alternates in sign from one parallel platelet to the next, as shown by $\tau = \sigma_{xx}/\sqrt{6}$, because the stress σ_{xx} alternates from tension to compression for adjacent Ni-rich and Cu-rich platelets.

For slip to occur, dislocations must pass through intertwined platelets of three orientations as shown by Butler and Thomas,[10] Ham, *et al*[11] and in Fig. 3. Dislocations with $\mathbf{a}/2\,[10\bar{1}]$ Burgers vectors are inhibited, *i.e.* pushed backwards (negative shear stress) by (001) platelets in compression ($\tau = \sigma_{xx}/\sqrt{6}$) and by (100) platelets in tension ($\tau = -\sigma_{xx}/\sqrt{6}$). Platelets oriented parallel to (010) do not influence $\mathbf{a}/2\,[10\bar{1}]$ dislocations because $\tau = 0$. Extensive bowing of dislocations through regions where $\tau = 0$ does not occur because the platelets of the three possible orientations are intertwined (Fig. 3). Dislocation radii of curvature due to the internal coherency stresses were calculated[5] to be 200 to 350Å for the aging conditions used in the present study, but the platelets were only 60 to 130Å thick (Fig. 2). Dislocations with such large radii of curvature relative to the precipitate platelet thickness would appear relatively straight as the curvature changed direction from platelet to platelet, and indeed relatively straight dislocations were observed in transmission electron micrographs of aged Cu-Ni-Fe alloys by Ham, Kirkaldy and Plewes.[11] Dislocations appear wavy only for Cu-Ni-Fe alloys aged to have much thicker platelets, *e.g.* 300Å thick.[10]

For yielding deformation to occur, dislocations must be generated at a source and move outward

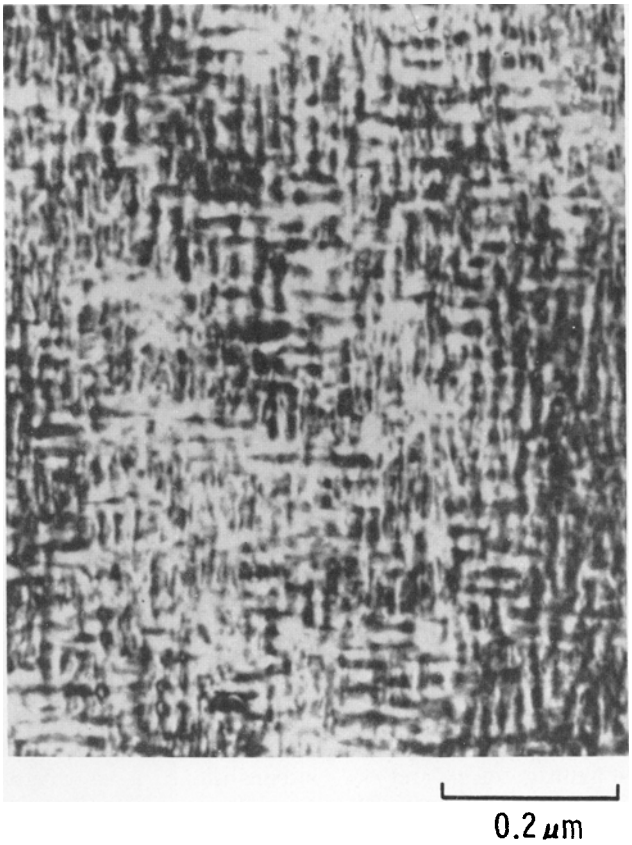

Fig. 3—Micrograph of Alloy 4 aged 15 min at 775°C showing the intertwined nature of precipitate platelets in aged Cu-Ni-Fe alloys. The micrograph was obtained by E. P. Butler and G. Thomas.[10] (Photo courtesy of Acta Metallurgica.)

as loops until the applied stress pushes them completely across a grain. Dislocations will experience no net force if they cross platelets[5] or are oriented parallel to those platelets that exert no shear stress, *e.g.* (010) platelets interacting with $\mathbf{a}/2\,[10\bar{1}]$ dislocations. Portions of dislocation loops oriented parallel to platelets that exert a shear stress, however, will be trapped between phases[5] and will be inhibited by the phase that exerts a retarding shear stress; the stress will be retarding for Phase 1 for one platelet orientation and retarding in Phase 2 for the second platelet orientation. The third platelet orientation will exert no resistance.

Dislocation segments in the loop that are adjacent to trapped segments but are not parallel to the platelets will move until they too become parallel to the platelets and also are trapped. Thus the length of dislocation trapped between phases continuously increases until the entire loop is immobilized. The stress to move immobilized dislocations then will depend on the shear stress in the retarding phase. Thus half the dislocations will be retarded by the shear stresses in Phase 1 and the other half will be retarded by the shear stress in Phase 2. Straight dislocations that are trapped at platelet boundaries will not be trapped over their entire length, however, because individual platelets of one orientation are intersected by platelets of other orientations that exert no net force on the dislocation. A straight dislocation parallel to platelets in Fig. 3, for example, thus would appear to be trapped over about 2/3 of its

length. Consequently, for yielding to occur, the average applied stress will be

$$\tau_{app} = \tau_f + \left(\frac{1}{2}\right)\left(\frac{2}{3}\right)|\tau_1| + \left(\frac{1}{2}\right)\left(\frac{2}{3}\right)|\tau_2|, \quad [3]$$

where τ_f is a frictional stress, τ_1 is the absolute value of the shear stress for platelets in tension (Phase 1) and τ_2 is the absolute value of the shear stress for platelets in compression (Phase 2). The two 1/2 factors in Eq. [3] arise because half of the dislocations are retarded by one phase and half by the other.

Upon substituting $\tau_1 = \sigma_{xx1}/\sqrt{6}$ and $\tau_2 = -\sigma_{xx2}/\sqrt{6}$ (the sign is changed because σ_{xx2} is compressive and therefore negative) for the shear stresses, Eq. [3] becomes

$$\tau_{app} = \tau_f + (\sigma_{xx1} - \sigma_{xx2})/3\sqrt{6}. \quad [4]$$

The equations for the stresses and strains (Eqs. [1] and [2]) can be substituted in Eq. [4], and although not necessary, the elastic stiffness constants are assumed to be the same in both phases. Thus

$$\tau_{app} = \tau_f + \frac{1}{3\sqrt{6}}\left(C_{11} + C_{12} - \frac{2C_{12}^2}{C_{11}}\right)\left(\frac{\bar{a} - a_{10}}{a_{10}} - \frac{\bar{a} - a_{20}}{a_{20}}\right). \quad [5]$$

The strains in Eq. [5] are small so it is permissible to approximate a_{10} and a_{20} in the denominator with a_0, the average of a_{10} and a_{20}. On consolidating the terms, $\bar{a}$ drops out in the numerator and

$$\tau_{app} = \tau_f + \frac{1}{3\sqrt{6}}\left(C_{11} + C_{12} - \frac{2C_{12}^2}{C_{11}}\right)\frac{\Delta a_0}{a_0}, \quad [6]$$

where $\Delta a_0 = a_{20} - a_{10}$. Eq. [6] indicates the yield strength is directly proportional to the difference in cubic lattice parameters and independent of all other parameters. The only term that was dependent on volume fraction, $\bar{a}$, dropped out and thus the equation indicates the yield strength is independent of volume fraction. Even though the volume fraction dependent term $\bar{a}$ drops out, Eq. [5] is instructive in showing which phase contributes the most to the magnitude of τ_{app}. It was found from earlier work[5] that the relative strain in each phase is inversely proportional to the volume fraction. Thus Eq. [5] shows that the larger strain in the thinner phase will contribute proportionally more to τ_{app} than the smaller strain in the thicker phase.

COMPARISON OF CALCULATED AND MEASURED YIELD STRENGTHS

Eq. [6] indicates the yield strength is proportional to Δa_0, and indeed plots of experimental yield strengths *vs* Δa_0 for Alloys 1 to 3 and Alloy 4 (Fig. 4) show just such a proportionality. Both plots extrapolate to zero at $\Delta a_0 = 0$, which indicates τ_f if quite small. An earlier analysis of age-hardening for similar systems by Cahn[9] indicated the yield strength would be proportional to the square of the coherency strain magnitude and also dependent upon particle spacing. Clearly, neither the coherency strain nor particle size dependencies observed in the present study fit Cahn's results. Maximum yield strengths obtained during the late stages of aging were studied for Cu-Ni-Fe, however, and Cahn's results probably fit much better during the early stages of aging when the yield strength is rapidly increasing, *e.g.* for 0 to 15 min at 625°C, Fig. 2. Other investigators[10,12] of the yield strength in Cu-Ni-Fe suggested an increase in yield strength magnitude with composition difference for a range of aging conditions, but no general relationship appeared to universally explain the yield strength for the complete range of aging treatments given their Cu-Ni-Fe alloys.[10,12] Lattice parameter differences are nearly proportional to composition differences for the alloys studied,[10,12] so their results indicated the yield strength magnitude also was approximately proportional to differences in lattice parameter, as observed in the present work for aging times that produced maximum yield strengths for a given aging temperature.

Tensile yield strengths were obtained using Eq. [6] and the equation, $\sigma_{yield} = \bar{m}\,\tau_{app}$, where $\bar{m}$ is the Taylor factor and is about 3.06 for polycrystalline samples with randomly oriented grains. Thus, assuming $\tau_f = 0$,

$$\sigma_{yield} = \frac{\bar{m}}{3\sqrt{6}}\left(C_{11} + C_{12} - \frac{2C_{12}^2}{C_{11}}\right)\frac{\Delta a_0}{a_0}. \quad [7]$$

Eq. [6] is equivalent to an equation previously reported[6,9] because $C_{11} + C_{12} - 2C_{12}^2/C_{11} = (S_{11} + S_{12})^{-1}$. Textured samples have different values for $\bar{m}$, and the samples tested in the present study were expected to have lower values for $\bar{m}$ because of a tendency to form a [100] fiber texture during processing. The value of $\bar{m}$ is 2.45 for [100] crystals.

Yield strengths were calculated for the Cu-Ni-Fe alloys for correlation with the experimentally measured yield strengths. Estimated elastic stiffness con-

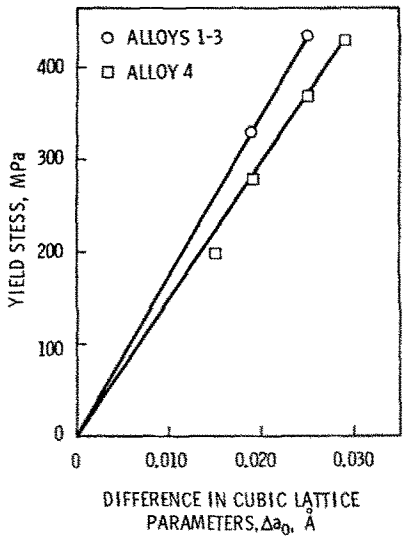

Fig. 4—Yield strength *vs* difference in cubic lattice parameters for Cu-Ni-Fe alloys aged to maximum yield strength at a given aging temperature. Individual points were measured experimentally and solid lines were calculated. Precipitate lattice parameters depended on precipitate compositions, which were established through the equilibrium diagram by aging temperature. Alloys 1 to 3 were selected on one tie line so the Cu-rich and Ni-rich precipitates in all three alloys had the same Cu-rich or Ni-rich composition for a given aging temperature. Moreover, the composition of each precipitate phase had the same dependency on aging temperature for all three alloys.

Table IV. Comparison of Yield Strengths Calculated from Eq. [7] with Measured Yield Strengths. Lattice Parameter Data Used to Determine Δa_0 were Taken from Refs. 7 and 13

Alloy	Aging Temperature, °C	Δa_0, Å	Yield Strength, MPa	
			Calculated	Measured
1 to 3	625	0.019	330	325
1 to 3	450	0.025	435	435
4	800	0.015	225	200
4	730	0.019	285	280
4	625	0.025	375	370
4	550	0.029	435	430

stants were (Ref. 6) $C_{11} = 2.2 \times 10^5$ MPa and $C_{12} = 1.5 \times 10^5$ MPa ($C_{11} + C_{12} - 2C_{12}^2/C_{11} = 1.65 \times 10^5$ MPa) for Alloys 1 to 3 and $C_{11} = 2.11 \times 10^5$ MPa and $C_{12} = 1.44 \times 10^5$ MPa ($C_{11} + C_{12} - 2C_{12}^2/C_{11} = 1.58 \times 10^5$ MPa) for Alloy 4. Lattice parameters used were $a_0 = 3.57$Å for Alloys 1 to 3 and $a_0 = 3.59$Å for Alloy 4 (Refs. 7, 13). Cubic lattice parameters for the precipitate phases depended only on precipitate compositions, which in turn depended on aging temperature. Lattice parameter data was obtained from Refs. 7 and 13 for evaluation of Δa_0 as a function of aging temperature as shown in Table IV and Fig. 4 for Alloys 1 to 3 and Alloy 4.

The best fit of the data using Eqs. [6] and [7] (Table IV) was obtained with $\overline{m} = 2.75$ for Alloys 1 to 3 and $\overline{m} = 2.5$ for Alloy 4, and the solid lines through the data points in Fig. 4 correspond to these values for $\overline{m}$. Using $\overline{m} = 2.75$ and 2.5 appropriately, $\sigma_{yield} = 1.73 \times 10^4$ (Δa_0) for Alloys 1 to 3 and $\sigma_{yield} = 1.5 \times 10^4$ (Δa) for Alloy 4. The processing for Alloy 4 (forged) was slightly different than for Alloys 1 to 3 (swaged), which would account for the observed difference in $\overline{m}$.

The elastic stiffness constants were assumed to be the same for both phases in the derivation of Eq. [7] from Eq. [4] and therefore also for the above calculations of yield strength. Results calculated previously[6] for the same Cu-Ni-Fe alloys using different estimated elastic stiffness constants for each phase justified the assumption because they were within the observed experimental accuracy of the results obtained in the present paper.

ACKNOWLEDGMENTS

The author wishes to thank Dr. M. D. Merz for reading the manuscript, Prof. G. Thomas and Dr. E. P. Butler for permission to use their micrograph, and Professors E. R. Parker and V. F. Zackay for their advice on the PhD thesis work.

This paper was based on a PhD Thesis entitled, *Calculation and Measurement of the Yield Stress of Alloys with Coherent Lamellar Microstructures*, by S. D. Dahlgren, University of California, Berkeley, CA, UCRL-16846, 1966. Work performed under the auspices of the U.S. Atomic Energy Commission and the Energy Research and Development Administration.

REFERENCES

1. V. Daniel and H. Lipson: *Proc. Roy. Soc.*, 1944, vol. A181, p. 378.
2. V. Daniel: *Proc. Roy. Soc.*, 1947, vol. 192, p. 575.
3. A. J. Bradley: *Proc. Phys. Soc.*, 1940, vol. 52, p. 80.
4. M. E. Hargreaves: *Acta Crystallogr.*, 1951, vol. 4, p. 301.
5. S. D. Dahlgren: *Met. Trans. A*, 1976, vol. 7A, p. 1661.
6. S. D. Dahlgren: PhD Thesis, UCRL Report No. 16846, University of California, Berkeley, Calif., 1966.
7. W. Köster and W. Dannöhl: *Z. Metallk.*, 1935, vol. 27, p. 220.
8. M. Hillert, M. Cohen, and B. L. Averbach: *Acta Met.*, 1961, vol. 9, p. 536.
9. J. W. Cahn: *Acta Met.*, 1963, vol. 11, p. 1275.
10. E. P. Butler and G. Thomas: *Acta Met.*, 1970, vol. 18, p. 347.
11. R. K. Ham, J. S. Kirkaldy, and J. T. Plewes: *Acta Met.*, 1967, vol. 15, p. 86.
12. R. J. Livak and G. Thomas: *Acta Met.*, 1971, vol. 19, p. 497.
13. A. J. Bradley, W. F. Cox, and H. J. Goldschmidt: *J. Inst. Metals*, 1941, vol. 67, p. 189.